

Supporting Information

Rationally Designed Fe-Tetrapyrrophenazine Complex: A Promising Precursor to Single-Atom Fe Catalyst for Efficient Oxygen Reduction Reaction in High-Power Zn-Air Cells

*Zheng Kun Yang,^{a,b} Cheng-Zong Yuan,^a and An-Wu Xu^{*a}*

^aDivision of Nanomaterials and Chemistry, Hefei National Laboratory for Physical Sciences at Microscale, University of Science and Technology of China, Hefei 230026, China

^bDepartment of Chemistry, University of Science and Technology of China, Hefei 230026, China

*To whom correspondence should be addressed.

Email: anwuxu@ustc.edu.cn

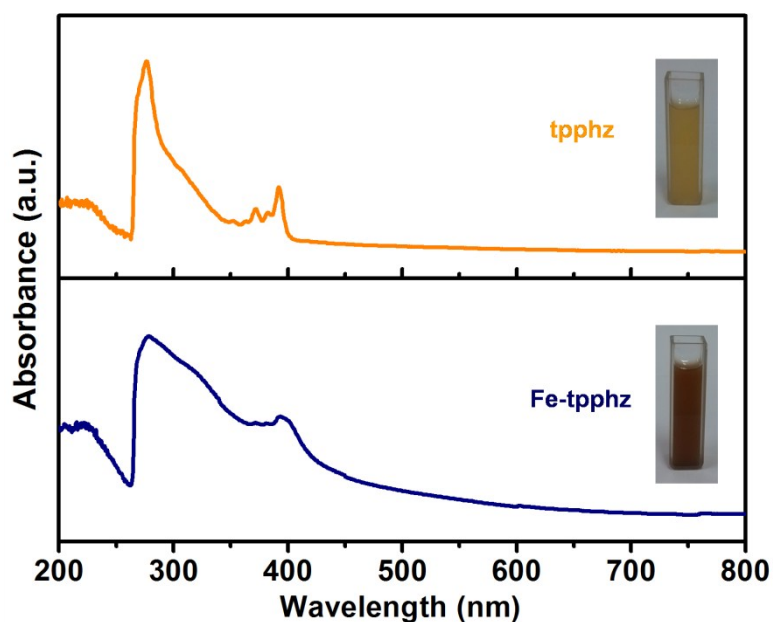


Fig. S1 UV-vis spectra of tpphz and Fe-tpphz measured in DMF solution. Inset: digital photo images of the tpphz and Fe-tpphz solution.

The yellow color of tpphz was observed. After adding Fe(II), its color immediately changed to brown. At higher energy, the spectrum of tpphz displays two sharp peaks (371 and 391 nm), corresponding to $n-\pi^*$ and transition. Below 350 nm, the strong band can be attributed to (tpphz) $\pi-\pi^*$. The disappearance of 371 nm peak was ascribed to the formation of Fe-N bonds. The higher absorption between 400 and 800 nm indicates the formation of Fe-tpphz complex.

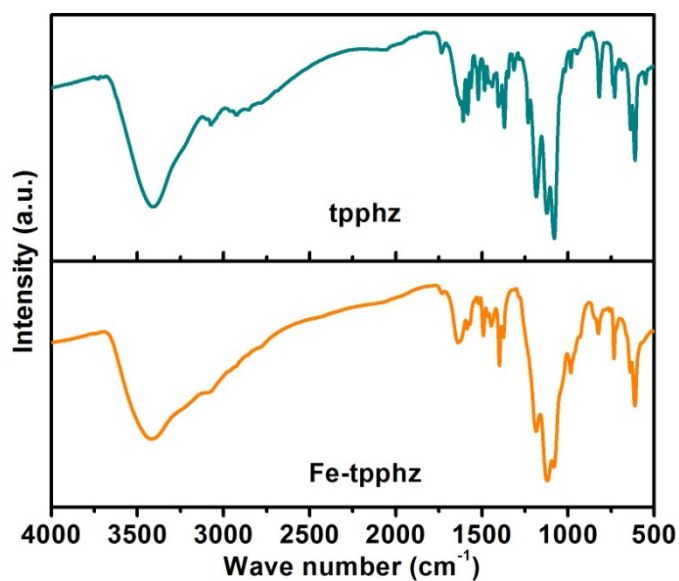


Fig. S2 FTIR spectra of tpphz and Fe-tpphz samples.

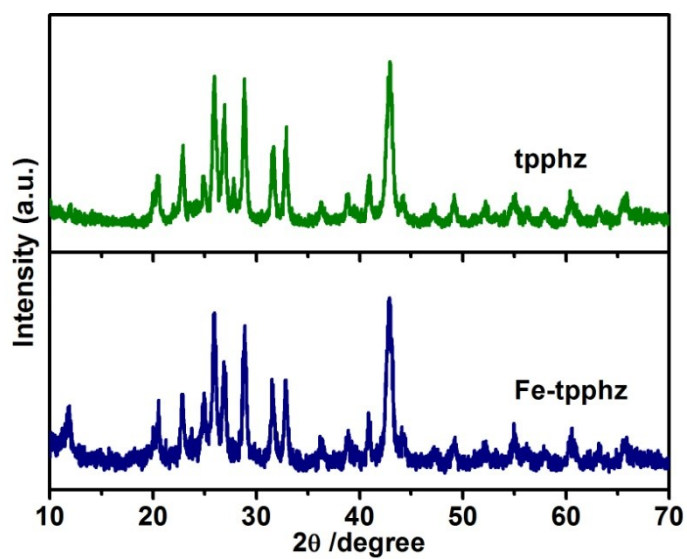


Fig. S3 XRD patterns of tpphz and Fe-tpphz samples.

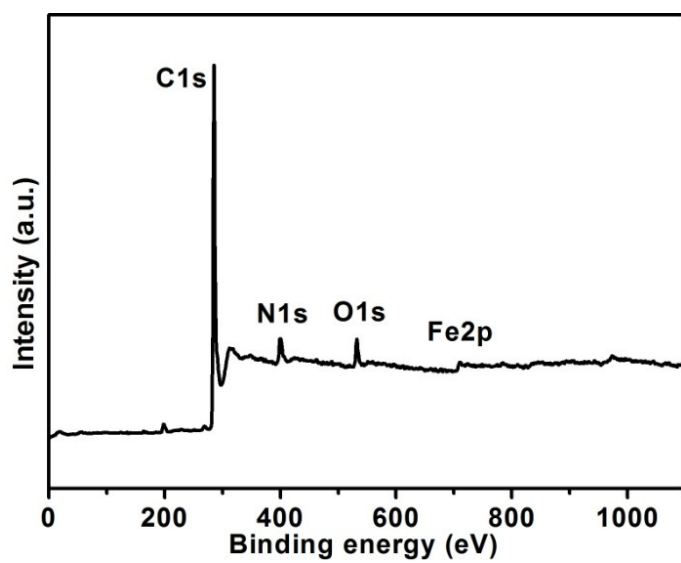


Fig. S4 XPS survey scan of Fe-N/C-700.

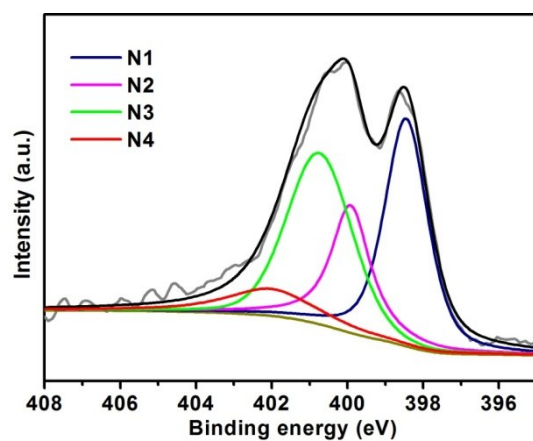


Fig. S5 N 1s XPS spectrum of the Fe-N/C-700 catalyst.

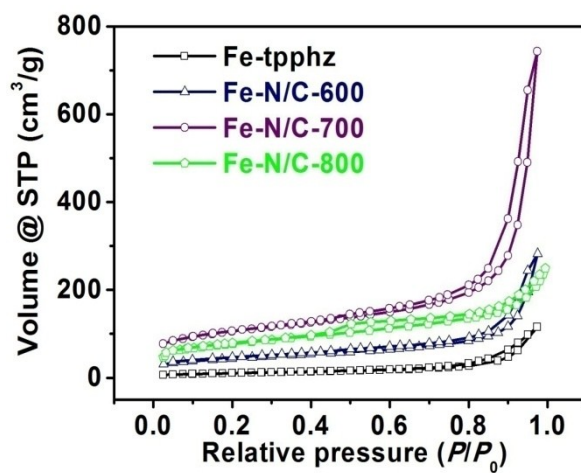


Fig. S6. N₂ adsorption/desorption isotherms of Fe-tpphz and Fe-N/C catalysts.

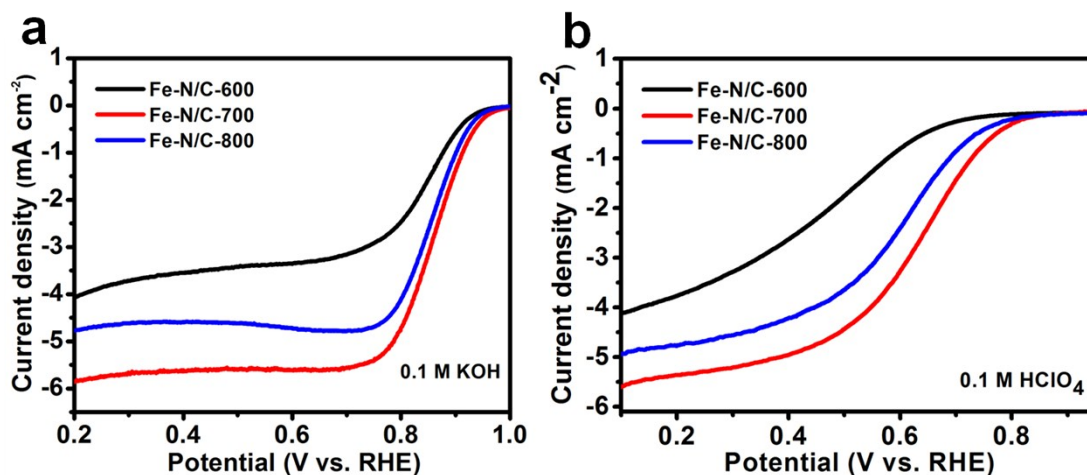


Fig. S7 LSV curves of Fe-N/C-x catalysts pyrolyzed at different temperatures in O₂-saturated 0.1 M KOH (a) and in O₂-saturated 0.1 M HClO₄ (b) solution with a sweep rate of 10 mV s⁻¹ and electrode rotation speed of 1600 rpm.

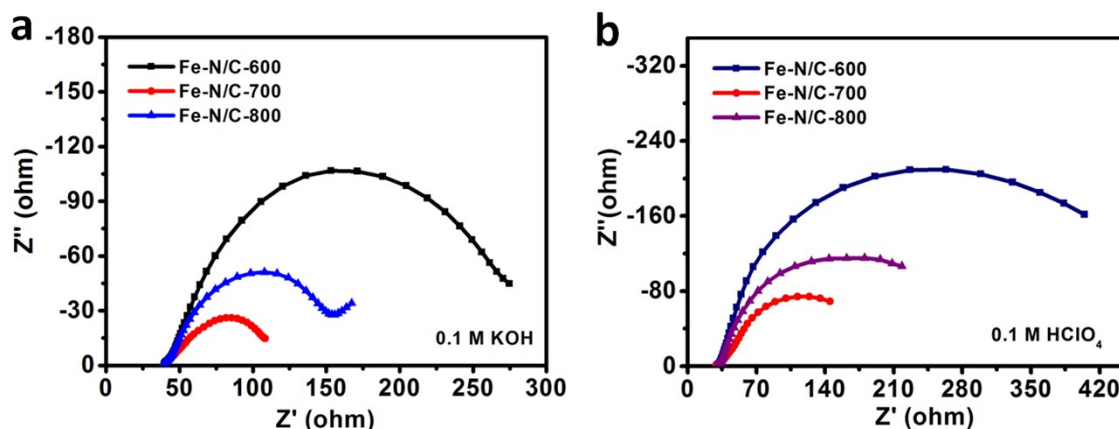


Fig. S8 Nyquist plots for Fe-N/C-x samples pyrolyzed at different temperatures in O₂-saturated 0.1 M KOH (a) and in O₂-saturated 0.1 M HClO₄ (b) solution.

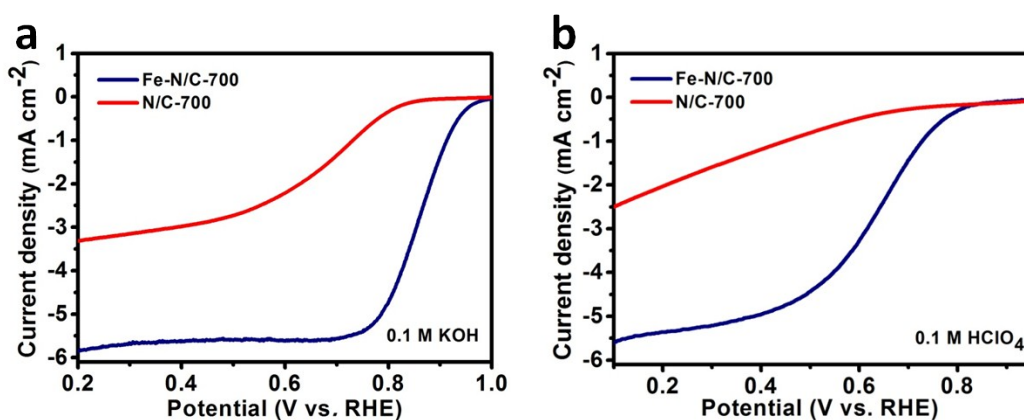


Fig. S9 LSV curves of pyrolyzed pure tpphz (N/C-700) catalyst and Fe-N/C-700 catalyst in O₂-saturated 0.1 M KOH (a) and 0.1 M HClO₄ (b) solution.

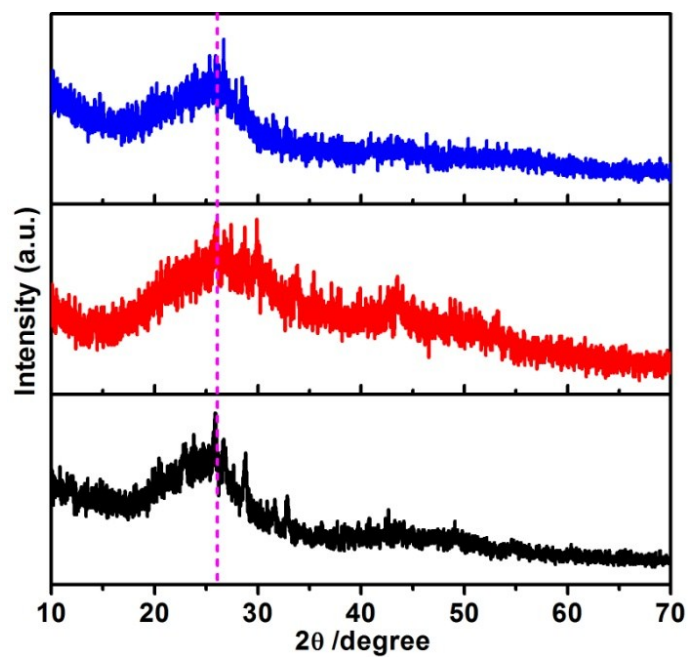


Fig. S10 XRD patterns of Fe-N/C catalysts pyrolyzed at different temperatures.

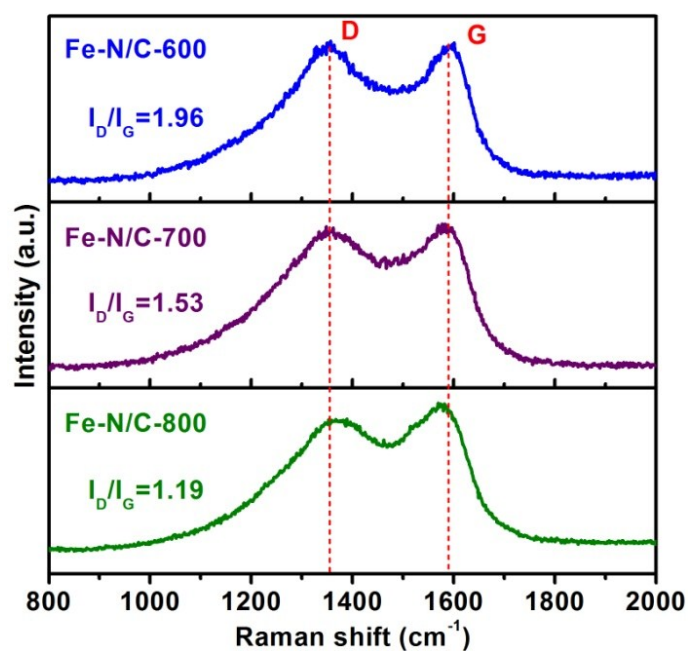


Fig. S11 Raman spectra of Fe-N/C catalysts pyrolyzed at different temperatures.

Table S1. Elemental compositions of Fe–N/C samples pyrolyzed at different temperatures determined by XPS.

Temp/°C	C atom %	N atom %	O atom %	Fe atom %
Fe-N/C-600	81.76	13.13	4.42	0.69
Fe-N/C-700	86.08	9.81	3.59	0.52
Fe-N/C-800	88.14	8.62	2.85	0.39

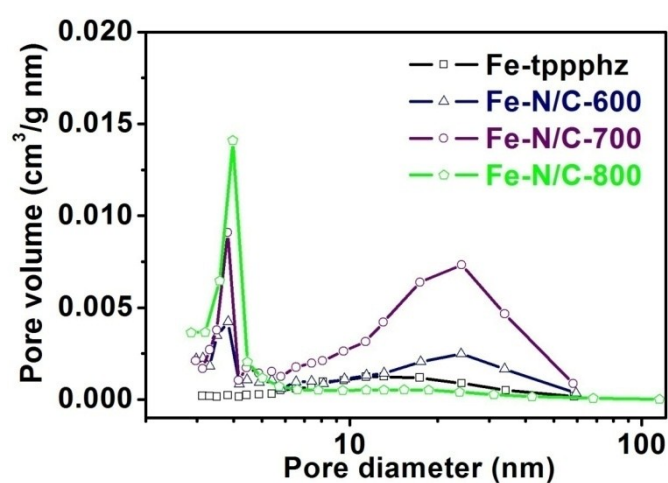


Fig. S12 Pore distribution of Fe-tpphz and Fe–N/C catalysts.

Table S2. Comparison of ORR performance for Fe-N/C-700 with other non-noble metal catalysts under alkaline condition from literature

Catalysts	Catalyst loading (mg cm ⁻²)	Onset potential (V vs RHE)	Current density (mA cm ⁻²)	Electron transfer numbers	Reference
Fe–N/C–700	0.15	0.98	5.8	4.0	This work
Fe@C-FeNC-2	0.7	0.98	5.3	4.0	J. Am. Chem. Soc. 2016, 138,

					3570. ChemSusChem 2014, 7, 1289.
P-Fe-N-CNFs	0.203	0.95	5.2	3.6	Adv. Mater., 2016, 28, 2337
LDH@ZIF-67-800	0.2	0.94	5.5	4.0	Adv. Mater., 2014, 26, 1450
CoP-CMP800	0.6	0.85	4.8	3.94	J. Mater. Chem. A 2014, 2, 8617.
PANI-4.5Fe-HT2(SBA-15)	0.61	0.95	4.5	3.4-4.0	J. Phys. Chem. C 2015, 119, 2583.
Fe/C/N	0.2	0.94	5.1	3.9	Angew. Chem. Int. Ed., 2015, 54, 8179
Fe-N-CNFs	0.6	0.93	5.12	3.95	Energy Environ. Sci., 2016, 9, 2563
Co₃(PO₄)₂C-N/rGOA	0.25	0.962	5.5	4.0	Angew. Chem. Int. Ed., 2015, 54, 12622
CoII-A-rG-O	0.6	0.88	5.3	3.95	Nature Energy, 2016, 1, 15006.
NCNTFs	0.2	0.95	5.2	3.97	Nanoscale, 2015, 7, 1501
Fe/N/C HNSs.	0.255	/	5.8	3.80	Angew. Chem. Int. Ed., 2013, 52, 5585
rGO/(Co²⁺-THPP)₇	1.0	0.86	4	3.85	Nanoscale, 2015, 7, 10334
Co-N-C-NS	0.464	0.93	5.7	3.7	

Fe/N/C	0.458	0.91	3.75	3.96	Sci. Rep., 2014, 4, 43866
Fe-Nx-C	0.36	0.95	5	3.3	Carbon, 214, 78-99
Fe ₃ C@NG800-0.2	0.2	0.95	5.5	3.5	ACS Appl. Mater. Interfaces, 2015, 7, 21511
Fe-N-C-900	0.2	0.88	5.6	4.0	Small, 2016, 12, 6398.
FeIM/ZIF-8	0.4	0.92	5.0	3.93	Chem. Sci., 2012, 3, 3200.

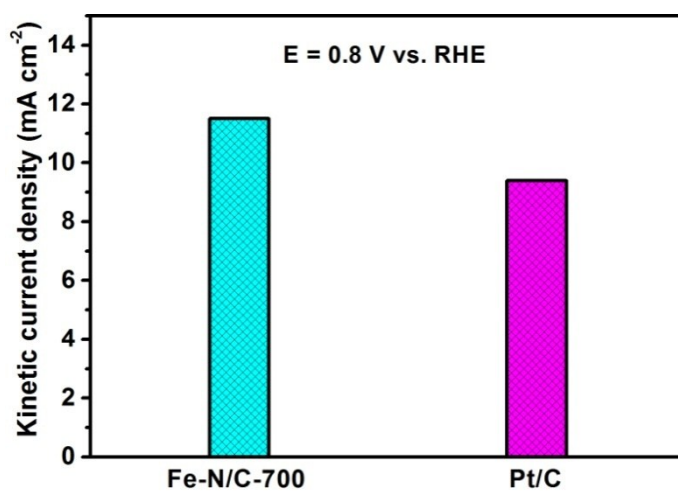


Fig. S13 Comparison of the kinetic current density normalized to electrode surface area of the catalysts measured at 0.8 V vs. RHE in O₂-saturated 0.1 M KOH solution.

Table S3. The Comparison of ORR performance of non-precious catalysts from the recent literature and this work (electrode 1600 rpm in 0.1 M HClO₄ medium)

Catalysts	loading mass (mg cm ⁻²)	Onset potential (V vs RHE)	Current density (mA cm ⁻²)	Electron transfer numbers	Reference

Fe-N/C-700	0.15	0.85	5.6	3.98	This work
FP-Fe-TA-N-850	0.3	0.83	5.5	3.5	Angew. Chem. Int. Ed., 2015, 54, 1
N-mesoporous carbon	0.8	0.80	4.5	3.2	J. Am. Chem. Soc., 2011, 133, 206
N,P-mesoporous nanocarbon	0.45	0.83	5.6	4.0	Nature Nanotech., 2015, 10, 444
Co/N/C	0.6	0.83	3.8	3.5	Chem. Eur. J., 2011, 17, 2063
Fe-N-C-750	0.6	0.89	4.05	3.96	ACS Catal., 2014, 4, 3928

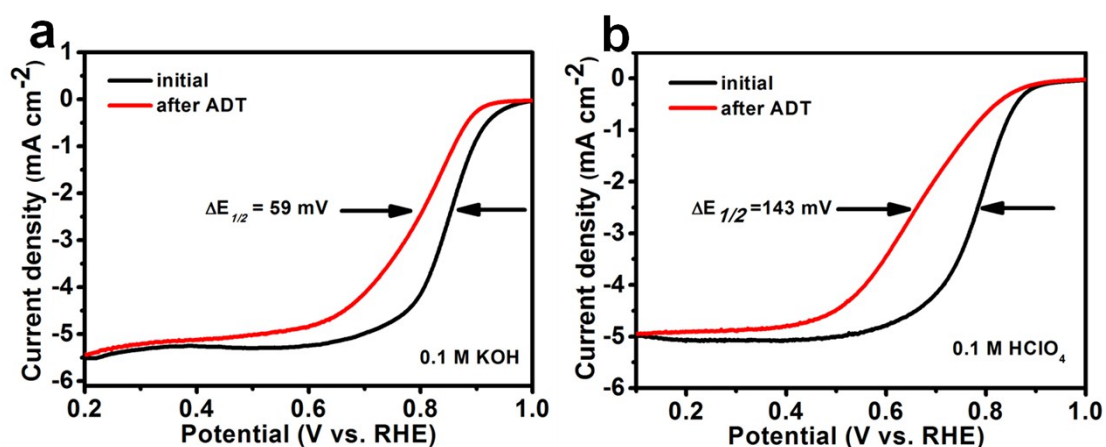


Fig. S14 LSV curves of Pt/C catalyst recorded before and after the ADT (8000 cycles) in O_2 -saturated 0.1 M KOH (a) and 0.1 M $HClO_4$ (b).

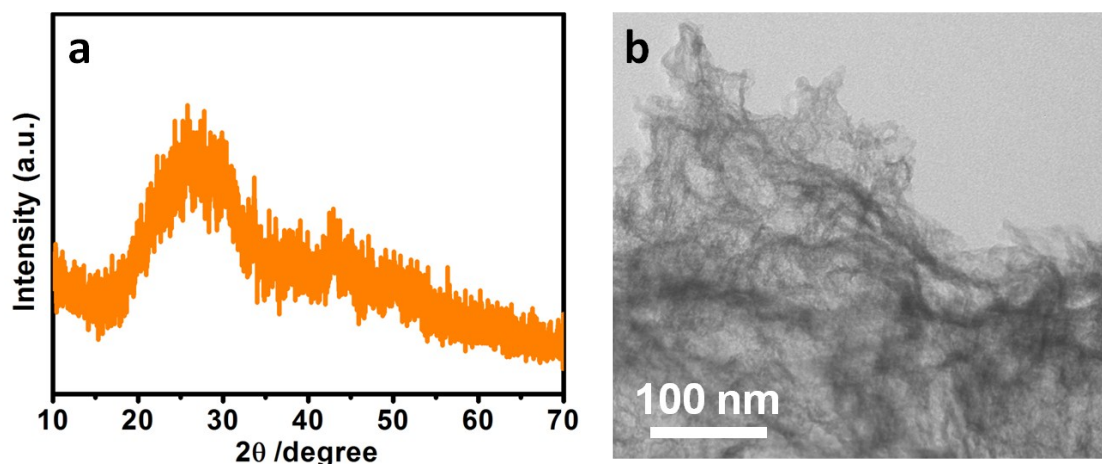


Fig. S15 The XRD pattern (a) and TEM image of the Fe-N/C-700 catalyst after the

ADT (8000 cycles).

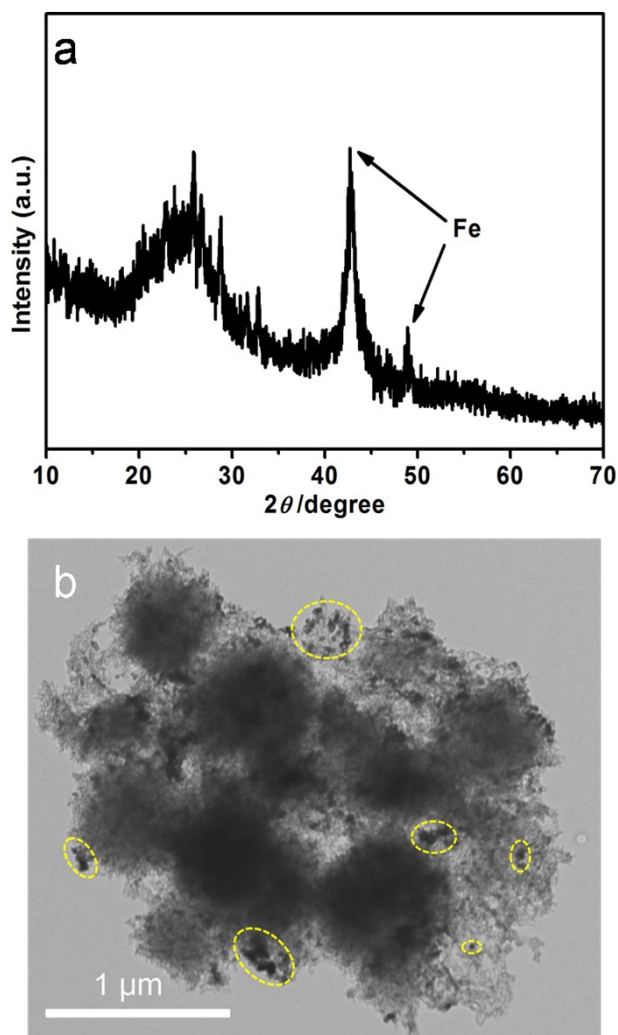


Fig. S16 XRD pattern (a) and TEM image (b) of Fe-N/C-700 catalyst before leaching in 6 M HCl solution.

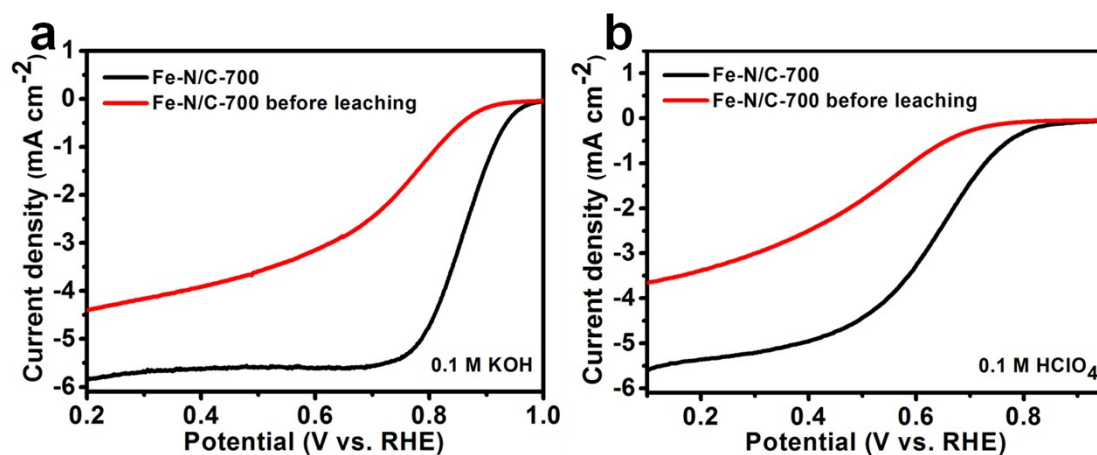


Fig. S17 LSV curves of Fe-N/C-700 catalyst in O₂-saturated 0.1 M KOH (a) and 0.1

M HClO₄ (b) before and after being leached in acid.

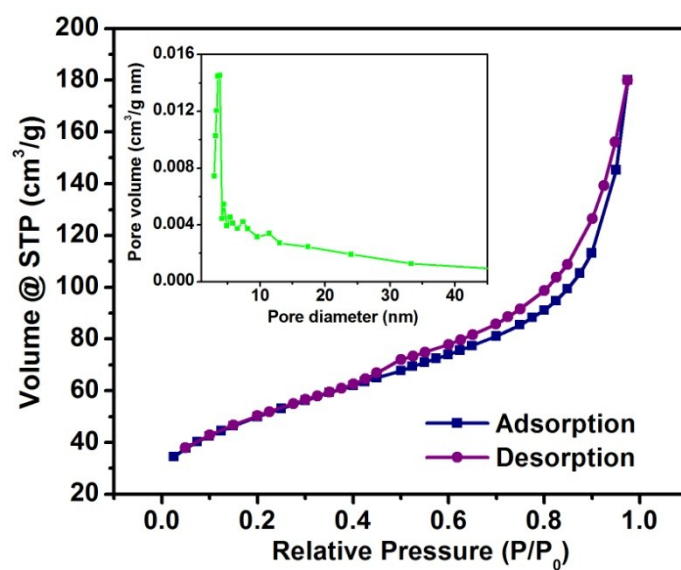


Fig. S18 N₂ adsorption/desorption isotherms of Fe-N/C-700 catalyst before etching and corresponding pore distribution (inset).

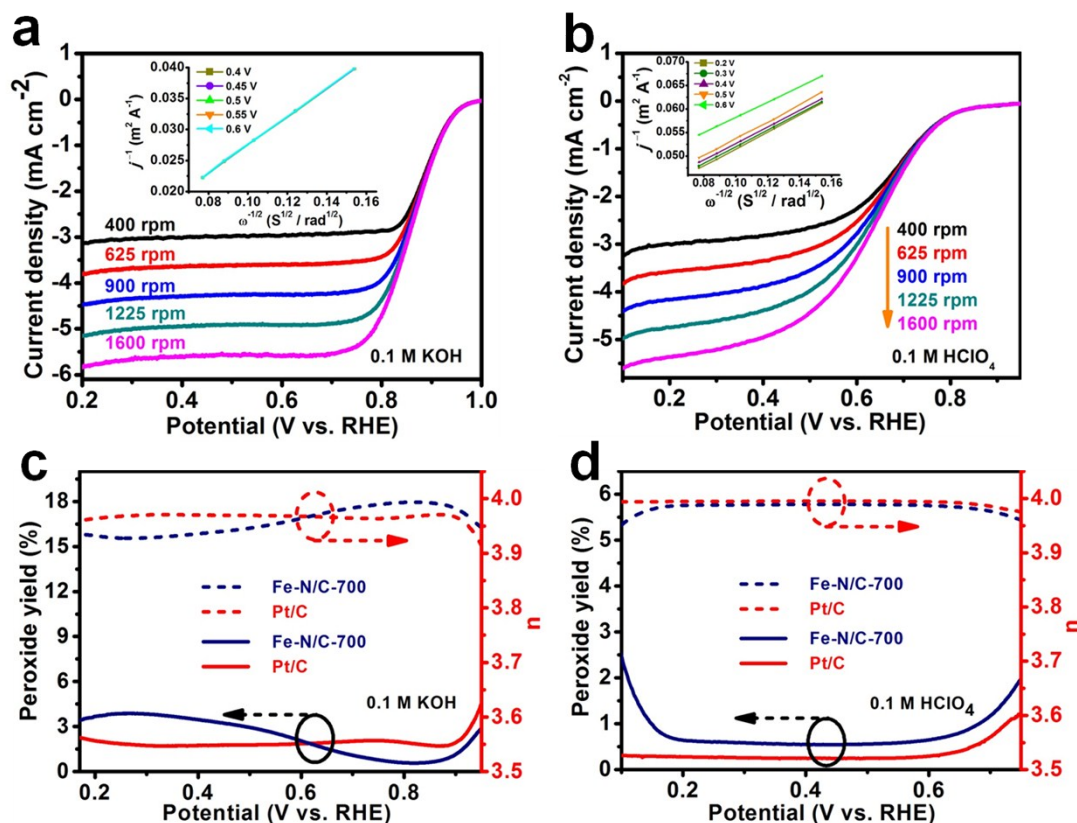


Fig. S19 (a) LSV curves of Fe-N/C-700 at different rotation rates in O₂-saturated 0.1 M KOH solution. Inset: the corresponding K-L plots at various potentials. (b) LSV curves of Fe-N/C-700 at different rotation rates in O₂-saturated 0.1 M HClO₄ solution. Inset: the corresponding K-L plots at various potentials. (c) Peroxide yield and the electron transfer number of the Fe-N/C-700 and Pt/C in O₂-saturated 0.1 M KOH. (d) Peroxide yield and the electron transfer number of the Fe-N/C-700 and Pt/C in O₂-saturated 0.1 M HClO₄.

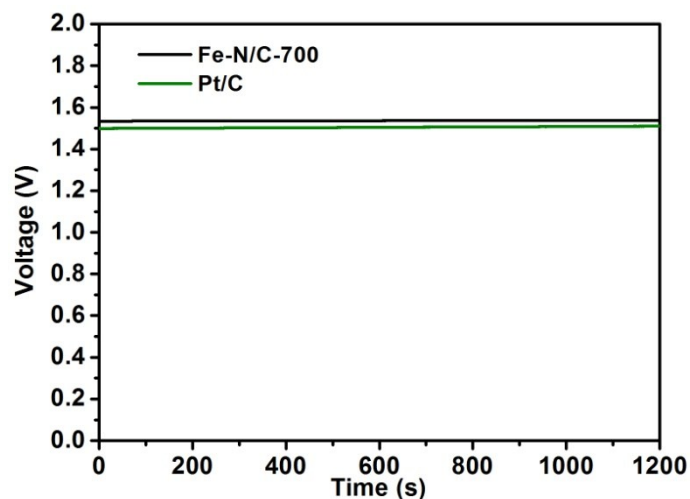


Fig. S20 The open circuit voltages of the Zn-air batteries using Fe-N/C-700 and commercial Pt/C as the cathode catalysts. The inset shows the schematic diagram of a primary Zn-air battery.

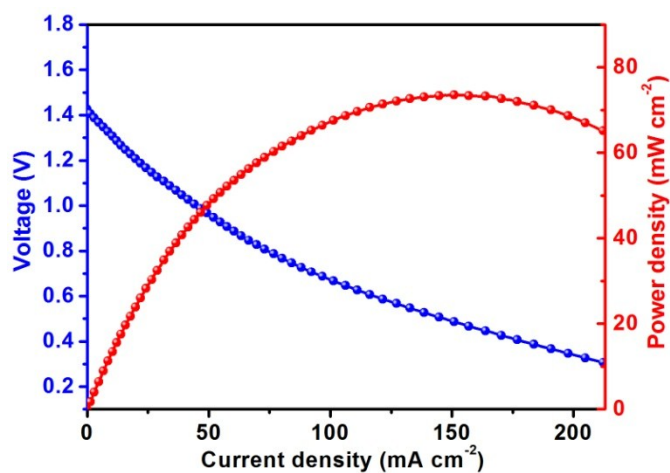


Fig. S21 The discharge polarization curve and corresponding power density of Zn-air cell using Fe-N/C-700 as the air catalyst.

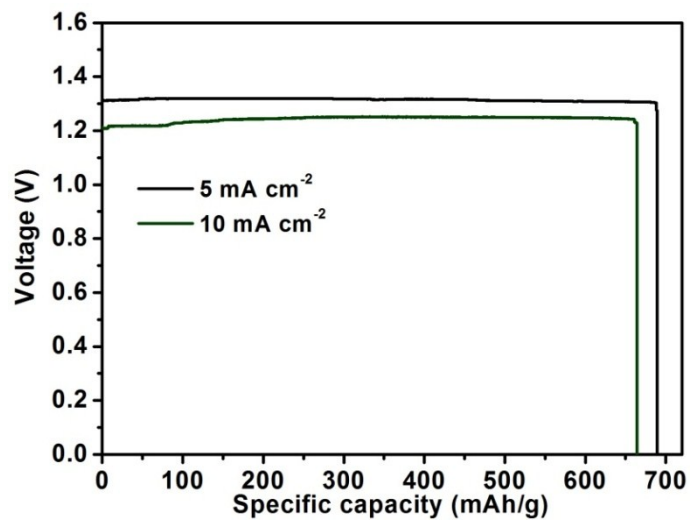


Fig. S22 Long-term galvanostatic discharge curves of Zn-air battery with Pt/C as cathode catalysts until complete consumption of the Zn anode. The specific capacity was normalized to the mass of consumed Zn anode.